ФИЗИКА ЭЛЕМЕНТАРНЫХ ЧАСТИЦ И АТОМНОГО ЯДРА
2015. Т. 46. ВЫП. 2

GEONEUTRINOS AND BOREXINO

L. Ludhova [a,*], *G. Bellini* [a], *J. Benziger* [k], *D. Bick* [s], *G. Bonfini* [e], *D. Bravo* [q], *B. Caccianiga* [a], *F. Calaprice* [l], *A. Caminata* [c], *P. Cavalcante* [e], *A. Chavarria* [l], *A. Chepurnov* [r], *D. d'Angelo* [a], *S. Davini* [t], *A. Derbin* [m], *A. Empl* [t], *A. Etenko* [g], *K. Fomenko* [b,e], *D. Franco* [h], *G. Fiorentini* [v], *C. Galbiati* [l], *S. Gazzana* [e], *C. Ghiano* [c], *M. Giammarchi* [a], *M. Göger-Neff* [n], *A. Goretti* [l], *C. Hagner* [s], *E. Hungerford* [t], *Aldo Ianni* [e], *Andrea Ianni* [l], *V. V. Kobychev* [f], *D. Korablev* [b], *G. Korga* [t], *D. Kryn* [h], *M. Laubenstein* [e], *B. Lehnert* [w], *T. Lewke* [n], *E. Litvinovich* [g], *F. Lombardi* [e], *P. Lombardi* [a], *G. Lukyanchenko* [g], *I. Machulin* [g], *S. Manecki* [q], *W. Maneschg* [i], *F. Mantovani* [v], *S. Marcocci* [c], *Q. Meindl* [n], *E. Meroni* [a], *M. Meyer* [s], *L. Miramonti* [a], *M. Misiaszek* [d], *P. Mosteiro* [l], *V. N. Muratova* [m], *L. Oberauer* [n], *M. Obolensky* [h], *F. Ortica* [j], *K. Otis* [p], *M. Pallavicini* [c], *L. Papp* [q], *L. Perasso* [c], *A. Pocar* [p], *G. Ranucci* [a], *A. Razeto* [e], *A. Re* [a], *B. Ricci* [v], *A. Romani* [j], *N. Rossi* [e], *R. Saldanha* [l], *C. Salvo* [c], *S. Schönert* [n], *H. Simgen* [i], *M. Skorokhvatov* [g], *O. Smirnov* [b], *A. Sotnikov* [b], *S. Sukhotin* [g], *Y. Suvorov* [u,g], *R. Tartaglia* [e], *G. Testera* [c], *D. Vignaud* [h], *R. B. Vogelaar* [q], *F. von Feilitzsch* [n], *H. Wang* [u], *J. Winter* [n], *M. Wojcik* [d], *A. Wright* [l], *M. Wurm* [s], *O. Zaimidoroga* [b], *S. Zavatarelli* [c], *K. Zuber* [w], *G. Zuzel* [d]

(Borexino Collaboration)

[a] Dipartimento di Fisica, Università degli Studi e INFN, Milano, Italy

[b] Joint Institute for Nuclear Research, Dubna

[c] Dipartimento di Fisica, Università e INFN, Genova, Italy

[d] M. Smoluchowski Institute of Physics, Jagellonian University, Cracow, Poland

[e] INFN Laboratori Nazionali del Gran Sasso, Assergi, Italy

*E-mail: Livia.Ludhova@mi.infn.it

[f] Kiev Institute for Nuclear Research, Kiev
[g] NRC Kurchatov Institute, Moscow
[h] APC, Univ. Paris Diderot, CNRS/IN2P3, CEA/Irfu, Obs. de Paris, Sorbonne, Paris
[i] Max-Planck-Institut für Kernphysik, Heidelberg, Germany
[j] Dipartimento di Chimica, Università e INFN, Perugia, Italy
[k] Chemical Engineering Department, Princeton University, Princeton, NJ, USA
[l] Physics Department, Princeton University, Princeton, NJ, USA
[m] St. Petersburg Nuclear Physics Institute, Gatchina, Russia
[n] Physik Department, Technische Universität München, Garching, Germany
[p] Physics Department, University of Massachusetts, Amherst, MA, USA
[q] Physics Department, Virginia Polytechnic Institute and State University, Blacksburg, VA, USA
[r] Skobeltsyn Institute of Nuclear Physics, Lomonosov Moscow State University, Moscow
[s] Institut für Experimentalphysik, Universität Hamburg, Hamburg, Germany
[t] Department of Physics, University of Houston, Houston, TX, USA
[u] Physics and Astronomy Department, University of California Los Angeles (UCLA), Los Angeles, CA, USA
[v] Dipartimento di Fisica e Scienze della Terra, Università degli Studi and INFN, Ferrara, Italy
[w] Institut für Kern- und Teilchenphysik, Technische Universität Dresden, Dresden, Germany

Geoneutrinos, electron antineutrinos produced in β-decays of naturally occurring radioactive isotopes in the Earth, are a unique direct probe of our planet's interior. After a brief introduction about the Earth, the geoneutrinos' properties and the main aims of their study are discussed. An overview of the latest experimental results obtained by the Borexino collaboration is provided, followed by a short overview of future perspectives of this new interdisciplinary field.

PACS: 91.80.+d; 23.40.-s; 14.60.Lm; 14.60.Cd

1. THE EARTH

The Earth was created in the process of accretion from undifferentiated material, to which chondritic meteorites are believed to be the closest in composition and structure. The bodies with a sufficient mass undergo the process of differentiation, e.g., a transformation from a homogeneous object into a body with a layered structure. The metallic core (3500 km radius) was the first to separate from the silicate primordial mantle which further differentiated into the current mantle (3000 km thickness) and the crust (from 5 to 75 km). The Fe–Ni metallic core with up to $\sim 10\%$ admixture of lighter elements, has a temperature range from 4100 to 5800 K. Its central part, inner core with the radius ~ 1300 km is solid due to high pressure. The 2200 km thick outer core is liquid and has a key role in the geodynamo process generating the Earth magnetic field. The D$''$ layer

is a core-mantle boundary, a 200 km thick seismic discontinuity of unclear origin. The lower mantle (2000 km) with a temperature gradient from 600 to 3700 K is solid, but viscose on long time scales. It is involved in the convection driving the movement of tectonic plates with a speed of few centimeters per year. A transition zone in the depth of 400–600 km is a seismic discontinuity due to mineral recrystallization. The upper mantle contains viscose astenosphere on which are floating the litospheric tectonic plates. These comprise the uppermost, rigid part of the mantle and the crust of two types: oceanic and continental. The continental crust (30 km average thickness) has the most complex history being the most differentiated and heterogeneous, consisting of igneous, metamorphic, and sedimentary rocks. The oceanic crust (5–10 km) is created along the mid-oceanic ridges where the basaltic magma differentiates from the partially melting mantle. A schematic profile of the Earth structure can be found in Fig. 1.

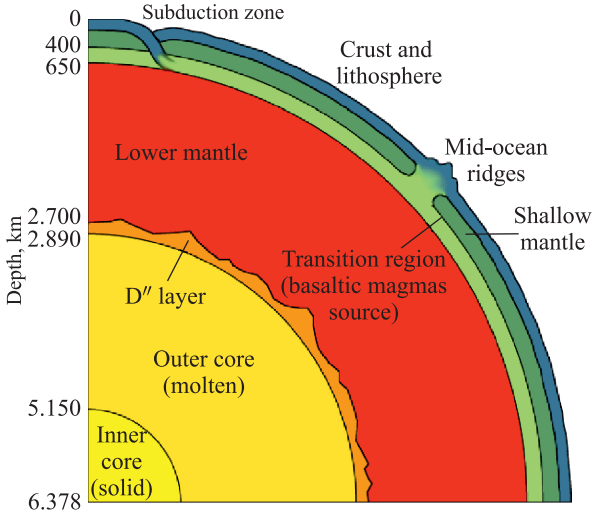

Fig. 1. A schematic profile of the Earth structure (from http://www.homepages.ucl.ac.uk/ ucfbdxa/resint.htm)

The bulk composition of the silicate Earth, the so-called Bulk Silicate Earth (BSE) models describe the composition of the Primitive Mantle, the Earth composition after the core separation and before the crust-mantle differentiation. The estimates of the composition of the present-day mantle can be derived as a difference between the mass abundances predicted by the BSE models in the Primitive Mantle and those observed in the present crust. In this way, the predictions of the U and Th mass abundances in the mantle are made, which are then critical in calculating the geoneutrino signal.

The most recent BSE-models classification is that of Šrámek et al. [1]:

• *Geochemical BSE models*. These models rely on the fact that the composition of carbonaceous (CI) chondrites matches the solar photospheric abundances in refractory lithophile, siderophile, and volatile elements. These models assume that the ratios of Refractory Lithophile Elements (RLE) in the bulk silicate Earth are the same as in the CI chondrites and in the solar photosphere. The typical chondritic value of the bulk mass Th/U ratio is 3.9 and K/U $\sim 13,000$. Among these models are McDonough and Sun (1995) [4], Allégre (1995) [5], Hart and Zindler (1986) [6], Arevalo et al. (2009) [7], and Palme and O'Neill (2003) [8]. The typical U concentration in the BSE is about (20 ± 4) ppb.

• *Cosmochemical BSE models*. The model of Javoy et al. (2010) [9] builds the Earth from the enstatite chondrites, which show the closest isotopic similarity with mantle rocks and have sufficiently high iron content to explain the metallic core (similarity in oxidation state). The "collisional erosion" model of O'Neill and Palme (2008) [10] is covered in this category as well. In this model, the early enriched crust was lost in the collision of the Earth with an external body. In both of these models the typical bulk U concentration is about 10–12 ppb.

• *Geodynamical BSE models*. These models are based on the mantle-convection energetics. Considering the current surface heat flux, which depends on the radiogenic heat and the secular cooling, the parameterized convection models require higher contribution of radiogenic heat (and thus higher U and Th abundances) with respect to geo- and cosmochemical models. The typical bulk U concentration is (35 ± 4) ppb.

The Earth surface heat flux is estimated based on the measurements of temperature gradients along several thousands of drill holes along the globe. The most recent evaluation of these data leads to the prediction of (47 ± 2) TW predicted by Davies and Davies (2010) [11], consistent with the estimation of Jaupart et al. (2007) [12]. The relative contribution of the radiogenic heat from radioactive decays to this flux (the so-called Urey ratio) is not known and this is the key information which can be pinned down by the geoneutrino measurements. The geochemical, cosmochemical, and geodynamical models predict the radiogenic heat of (20 ± 4), (11 ± 2), (33 ± 3) TW and the corresponding Urey ratios of about 0.3, 0.1, and 0.6, respectively. The Heat Producing Elements (HPE) predicted by these models are distributed in the crust and in the mantle. The crustal radiogenic power was recently evaluated by Huang et al. [3] as $6.8^{+1.4}_{-1.1}$ TW. By subtracting this contribution from the total radiogenic heat predicted by different BSE models, the mantle radiogenic power driving the convection and plate tectonics can be as little as 3 TW and as much as 23 TW. To determine this mantle contribution is one of the main goals and potentials of Neutrino Geoscience, a new inter-disciplinar field studying geoneutrinos.

2. GEONEUTRINOS

Geoneutrinos (geo-$\bar{\nu}_e$), electron antineutrinos ($\bar{\nu}_e$) are produced in β-decays of ^{40}K and of several nuclides in the chains of long-lived radioactive isotopes ^{238}U and ^{232}Th, which are naturally present in the Earth:

$$^{238}\mathrm{U} \rightarrow {}^{206}\mathrm{Pb} + 8\alpha + 8e^- + 6\bar{\nu}_e + 51.7 \text{ MeV}, \quad (1)$$

$$^{232}\mathrm{Th} \rightarrow {}^{208}\mathrm{Pb} + 6\alpha + 4e^- + 4\bar{\nu}_e + 42.8 \text{ MeV}, \quad (2)$$

$$^{40}\mathrm{K} \rightarrow {}^{40}\mathrm{Ca} + e^- + \bar{\nu}_e + 1.32 \text{ MeV}. \quad (3)$$

The Earth shines in geoneutrinos with a flux of about 10^6 cm$^{-2} \cdot$ s^{-1}. It is important to note that the ratio of the released radiogenic heat and the geoneutrino flux is in a well fixed and known ratio. Therefore, it is in principle possible to determine the Urey ratio by measuring the geoneutrino flux. By measuring the geoneutrino flux at different locations through the globe, in different geological settings and/or by being able to identify the incoming direction of detected geoneutrinos, it might be possible to:

- study the distribution of radioactive elements within the Earth, to determine their abundances in the crust and in the mantle;
- determine if there are any radioactive elements in the Earth core;
- understand if the mantle composition is homogeneous or not;
- test, validate, and discriminate among different BSE models;
- exclude or confirm the presence of the georeactor in the core;
- determine the Urey ratio, important for geochemistry and geophysics;
- to study the bulk U and Th ratio in the sillicate Earth, an important parameter for geochemistry which could shed light on the process of the Earth formation.

We can see that geoneutrinos can be used as a unique direct probe of the Earth interior, not accessible by any other means. All this information could be used as inputs for many geological, geophysical, and geochemical models describing such complex processes as the mantle convection, movement of tectonic plates, geodynamo (the process of the generation of the Earth magnetic field), the process of the Earth formation, etc. . .

The energy spectrum of geoneutrinos extends to about 3.3 MeV. They are detected via the inverse neutron β-decay reaction

$$\bar{\nu}_e + p \rightarrow e^+ + n, \quad (4)$$

which has a kinematic threshold of 1.806 MeV. The cross section of this interaction as a function of antineutrino energy is well known and can be found in [13]. Unfortunately, all geoneutrinos produced in the decay of ^{40}K are below this threshold and we are able to detect only the tail of the ^{238}U and ^{232}Th

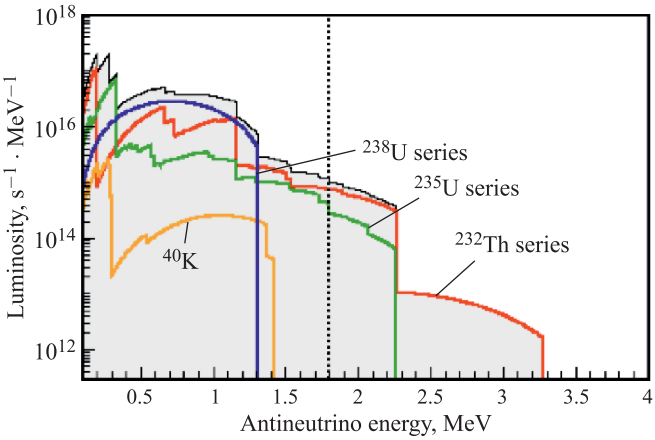

Fig. 2. The geoneutrino luminosity as a function of energy is shown for the most important reaction chains and nuclides [14]. Only geoneutrinos of energies above the 1.8 MeV energy (vertical dashed line) can be detected by means of the inverse β-decay on target protons shown in Eq. (4)

geoneutrinos, as shown in Fig. 2. Geoneutrinos from the ^{232}Th chain have the end point of their energy spectrum at about 2.25 MeV, while those from the ^{238}U chain extend up to 3.3 MeV. Ideally, this spectral feature could be used in order to measure the U and Th ratio in the Earth. It is important to recall, that the relative proportions of the elements abundances are much better known than their absolute abundances. Therefore, by measuring the absolute abundances of ^{238}U and ^{232}Th, the absolute abundance of ^{40}K can be deduced with a better precision.

Geoneutrinos are emitted and interact as flavor states but they travel as superposition of mass states and are, therefore, subject to flavor oscillations. In the approximation $\Delta m^2_{31} \sim \Delta m^2_{32} \gg \Delta m^2_{21}$, the square-mass differences of mass eigenstates 1, 2, 3, the survival probability P_{ee} for a $\bar{\nu}_e$ in vacuum are

$$P_{ee} = P(\bar{\nu}_e \to \bar{\nu}_e) = \sin^4\theta_{13} + \\ + \cos^4\theta_{13}\left(1 - \sin^2 2\theta_{12}\sin^2\left(\frac{1.267\Delta m^2_{21}L}{4E}\right)\right). \quad (5)$$

In the Earth, the geoneutrino sources are spread over a vast region compared to the oscillation length

$$L \sim \pi c\hbar\frac{4E}{\Delta m^2_{21}}. \quad (6)$$

For example, for a $\sim$ 3 MeV antineutrino, the oscillation length is $\sim$ 100 km, small with respect to the Earth radius of $\sim$ 6371 km: the effect of the neutrino

oscillation to the total neutrino flux is well averaged, giving an overall survival probability of

$$\langle P_{ee} \rangle \simeq \cos^4 \theta_{13} \left(1 - \frac{1}{2} \sin^2 2\theta_{12} \right) + \sin^4 \theta_{13}. \quad (7)$$

According to the neutrino oscillation mixing angles and square-mass differences reported in [15], $P_{ee} \sim 0.54$. It has been calculated in [16] that the so-called *matter effect* contribution to the average survival probability is an increase of about 2% and the spectral distortion is below 1%. To conclude, the net effect of flavor oscillations during the geoneutrino ($\bar{\nu}_e$) propagation through the Earth is an absolute decrease of the overall flux by ~ 0.55 with a very small spectral distortion, negligible for the precision of the current geoneutrino experiments.

3. LATEST GEONEUTRINO RESULTS FROM BOREXINO

There are only two running experiments able to measure geoneutrinos: Borexino placed at the Laboratori Nazionali del Gran Sasso in central Italy and KamLAND in Kamioka mine in Japan. Both experiments are large-volume liquid-scintillator detectors placed in the underground in order to shield from cosmic rays. Borexino and KamLAND are placed in very different geological environments and are also very far from each other. Borexino is placed on a continental crust while KamLAND in a complicated subduction region at the border of oceanic and continental crusts. The measurements from both experiments are therefore complementary and probing different geological settings, and they could shed light on the hypothesis of a homogeneous vs. heterogeneous mantle.

The first experimental indication of a geoneutrino measurement ($\sim 2.5\sigma$ C.L.) was reported by the KamLAND collaboration [17] and [18]. The observation of geoneutrinos at 99.997% C.L. was then achieved by both Borexino [19] and KamLAND [20]. In March 2013, both experiments updated their geoneutrino measurements. KamLAND [21] came up with a reactor on-off study of backgrounds and an improved sensitivity to $\bar{\nu}_e$, possible because all Japanese nuclear reactors were temporarily switched off for a safety review after the Fukushima nuclear accident occurred in March 2011. The KamLAND results are described in a dedicated contribution of KamLAND collaboration, while here we describe the latest Borexino update [22].

3.1. Borexino Detector. The Borexino detector is located under the Gran Sasso mountain in the hall C of the Laboratori Nazionali del Gran Sasso (LNGS) in central Italy. It is an unsegmented liquid scintillator detector built for the spectral measurement of low-energy solar neutrinos. Several calibration campaigns with radioactive sources [23] allowed us to decrease the systematic errors of the

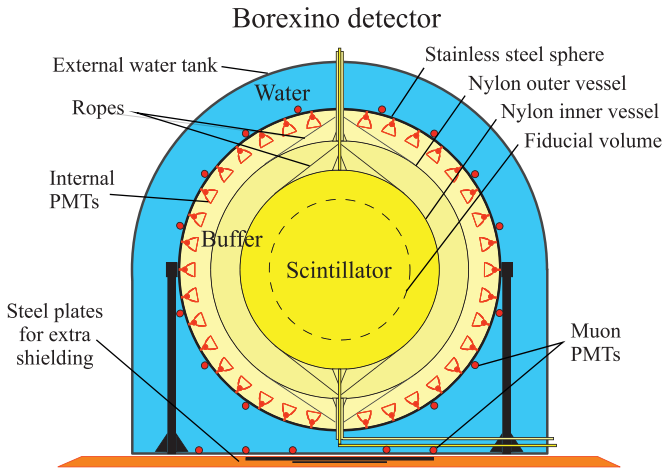

Fig. 3. Schematic view of the Borexino detector

measurements and to optimize the full GEANT4 Monte-Carlo (MC) simulation. The 278 t of ultrapure liquid scintillator (pseudocumene (PC) doped with 1.5 g/l of diphenyloxazole) are confined within a thin spherical nylon vessel with a radius of 4.25 m. The detector core is shielded from external radiation by 890 t of buffer liquid, a solution of PC and 3–5 g/l of the light quencher dimethylphthalate. The buffer is divided into two volumes by the second nylon vessel with a 5.75 m radius, preventing inward radon diffusion. All this is contained in a 13.7 m diameter stainless steel sphere (SSS) on which are mounted 2212 8" PMTs detecting the scintillation light, the so-called Inner Detector. An external, domed water tank of 9 m radius and 16.9 m height, filled with ultrahigh purity water, serves as a passive shield against neutrons and gamma rays as well as an active muon veto. The Cherenkov light radiated by muons passing through the water is measured by 208 8" external PMTs also mounted on the SSS and defines the so-called Outer Detector. For more details concerning the Borexino detector see [24, 25].

3.2. Results. The Borexino result [22] refers to the statistics collected from December 2007 to August 2012 corresponding to 1352.60 days of lifetime. The fiducial exposure after all cuts is (613 ± 26) t $\cdot$ y or $(3.69 \pm 0.16) \cdot 10^{31}$ proton $\cdot$ y.

Electron antineutrinos are measured through inverse neutron β-decay reaction of Eq. (4). The positron created in this reaction promptly comes to rest and annihilates. All deposited energy is detected in a single prompt event, with a visible energy of $E_{\mathrm{prompt}} = E_{\bar{\nu}_e} - 0.784$ MeV. The emitted free neutron is typically captured on protons, resulting in the emission of a 2.22 MeV de-excitation

γ ray, providing a delayed coincidence event. The mean neutron-capture time in Borexino was measured with an AmBe neutron source to be $\tau = (254.5 \pm 1.8)$ μs. The characteristic time and spatial coincidence of prompt and delayed events offers a clean signature of $\bar{\nu}_e$ detection, further suppressing possible background sources.

The $\bar{\nu}_e$'s from nuclear power plants are the main antineutrino background to the geoneutrino measurement. Since there are no nuclear plants close-by, the LNGS site is well suited for geoneutrino detection. The number of expected reactor $\bar{\nu}_e$ candidates is $N_{\mathrm{react}} = (33.3 \pm 2.4)$ events after cuts. Thanks to the extreme radiopurity of the Borexino detector, the non-antineutrino background is almost negligible: only (0.7 ± 0.18) events, dominated by $\beta+$neutron decays of cosmogenic ^{9}Li and ^{8}He, accidental coincidences, and (α, n) reactions with α's from decays of ^{210}Po.

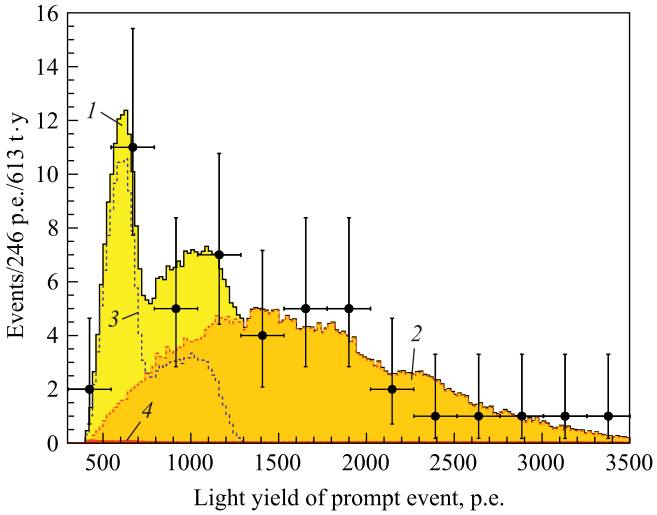

Fig. 4 (color online). Light yield spectrum of the 46 prompt golden antineutrino candidates and the best fit. The yellow area (*1*) isolates the contribution of the geo-$\bar{\nu}_e$ in the total signal. Dashed red line/orange area (*2*): reactor-$\bar{\nu}_e$ signal from the fit. Dashed blue line (*3*): geo-$\bar{\nu}_e$ signal resulting from the fit. The contribution of other background is almost negligible and is shown by the small red filled area (*4*) in the lower left part. The conversion from photoelectrons (p.e.) to energy is approximately 500 p.e./MeV

The Borexino collaboration selected 46 antineutrino candidates, the prompt energy spectrum of which is shown in Fig. 4. An unbinned maximal likelihood fit of the energy, expressed in light yield, spectrum of prompt candidates, was performed, with the Th/U mass ratio fixed to the chondritic value of 3.9, and with the number of events from reactor antineutrinos left as a free parameter.

Our best fit values are $N_{\rm geo} = (14.3 \pm 4.4)$ events and $N_{\rm react} = 31.2^{+7.0}_{-6.1}$ events, corresponding to signals $S_{\rm geo} = (38.8 \pm 12.0)$ TNU* and $S_{\rm react} = 84.5^{+19.3}_{-16.9}$ TNU. The measured geoneutrino signal corresponds to overall $\bar{\nu}_e$ fluxes from U and Th decay chains of $\phi({\rm U}) = (2.4 \pm 0.7) \cdot 10^6$ cm$^{-2} \cdot$ s^{-1} and $\phi({\rm Th}) = (2.0 \pm 0.6) \cdot 10^6$ cm$^{-2} \cdot$ s^{-1}. From the $\ln \mathcal{L}$ profile, the null geoneutrino measurement has a probability of $6 \cdot 10^{-6}$. The signal from the reactors is in full agreement with the expectations of (33.3 ± 2.4) events in the presence of neutrino oscillations.

3.3. Geological Implications. A contribution of the local crust (LOC) to the total geoneutrino signal, based on the local 3D geology around the LNGS laboratory, was carefully estimated in [26] as $S_{\rm geo}({\rm LOC}) = (9.7 \pm 1.3)$ TNU. The contribution from the Rest Of the Crust (ROC), based on the recent calculation by Huang et al. [3], results in the geoneutrino signal from the crust (LOC + ROC) of $S_{\rm geo}({\rm Crust}) = (23.4 \pm 2.8)$ TNU. Subtracting the estimated crustal components from the Borexino geoneutrino rate, we can infer the contribution of the mantle, $S_{\rm geo}({\rm Mantle}) = (15.4 \pm 12.3)$ TNU. The current result cannot discriminate among the different BSE models.

The Earth releases radiogenic heat, $H_{\rm geo}$, together with geoneutrinos in a well fixed ratio, however the observed geoneutrino signal depends both on the abundances of the individual radioactive elements and on their distribution inside the Earth. To extract the radiogenic heat power from a measured $S_{\rm geo}$ is therefore model-dependent. We have calculated the expected $S_{\rm geo}({\rm U + Th})$ as a function of the radiogenic heat produced by U and Th, $H_{\rm geo}({\rm U + Th})$, see Fig. 5, and compared it to the results. The allowed regions between the red (*1*) and blue (*2*) lines in the plane $S_{\rm geo}({\rm U + Th})$ and $H_{\rm geo}({\rm U + Th})$ contain models consistent with geochemical and geophysical data. For each total mass of U and fixed Th/U ratio, the maximal geoneutrino signal (red line *1*) can be obtained by maximizing the radiogenic material in the crust and allowing uniform distribution in the mantle. Similarly, the minimal signal (blue line *2*) is obtained for the minimal radiogenic mass in the crust with the rest concentrated in a thin layer at the bottom of the mantle. The expected signal from the crust is taken from Table V of [27]. We have chosen as a reference the BSE model from [4], predicting that the silicate Earth contains $m(U) = (0.8 \pm 0.1) \cdot 10^{17}$ kg with mass ratios ${\rm Th/U} = 3.9$ and ${\rm K/U} = 12000$. The green regions (*3*) are allowed by this BSE model. The arrow "Min" indicates the contribution of the crust only. The arrow for the fully radiogenic model indicates 39.3 TW: it assumes that the total Earth surface heat flux of (47 ± 2) TW [11] is completely due to radiogenic heat from U, Th, and K. Taking the relative proportions from the BSE of [4], we get that in a fully radiogenic Earth, U, Th, and K produce 19.1, 20.2, and 7.7 TW, respectively.

*1 TNU = 1 Terrestrial Neutrino Unit = 1 event/y/10^{32} protons.

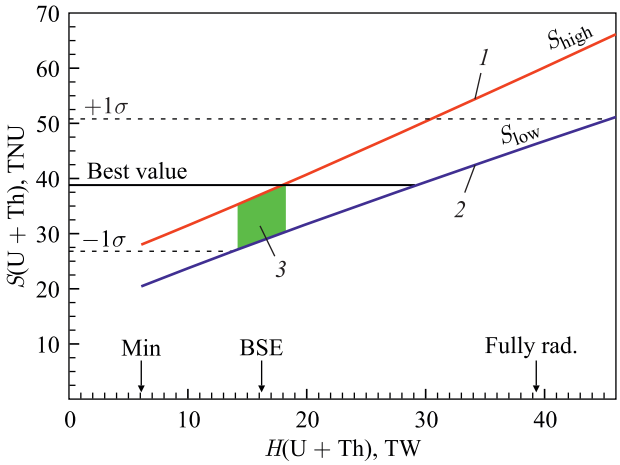

Fig. 5 (color online). The signal $S(\mathrm{U}+\mathrm{Th})$ from U and Th geoneutrinos as a function of radiogenic-heat production rate $H(\mathrm{U}+\mathrm{Th})$ in Borexino. Details in the text

We have performed another unbinned maximal likelihood fit of our 46 golden candidates in which the individual contributions from the ^{238}U and ^{232}Th chains were fitted individually. The best fit values are $N_{\mathrm{Th}} = (3.9 \pm 4.7)$ events and $N_{\mathrm{U}} = (9.8 \pm 7.2)$ events, corresponding to $S_{\mathrm{Th}} = (10.6 \pm 12.7)$ TNU and $S_{\mathrm{U}} = (26.5 \pm 19.5)$ TNU and $\bar{\nu}_e$ fluxes (above 0 MeV) of $\phi(\mathrm{Th}) = (2.6 \pm 3.1) \times 10^6$ cm$^{-2} \cdot$ s^{-1} and $\phi(\mathrm{U}) = (2.1 \pm 1.5) \cdot 10^6$ cm$^{-2} \cdot$ s^{-1}. Although our data is compatible within 1σ with only ^{238}U signal (and $S_{\mathrm{Th}} = 0$) or only ^{232}Th signal (and $S_{\mathrm{U}} = 0$), we note that the best fit of the Th/U ratio is in very good agreement with the chondritic value.

A georeactor with thermal power < 30 TW and $^{235}\mathrm{U} : {}^{238}\mathrm{U} = 0.76 : 0.23$ composition was suggested by Herndon [28]. It is assumed to be confined in the central part of the Earth core within the radius of about 4 km [29]. We have produced MC spectra of the expected georeactor antineutrino. In a similar unbinned maximal likelihood fit of our 46 golden antineutrino candidates we have added another fit component, N_{georeact}, while constraining N_{react} to the expected value of (33.3 ± 2.4) events. All other fit details were as above, including fixed chondritic mass Th/U ratio. We set the upper limit on the georeactor power 4.5 TW at 95% C.L.

4. FUTURE PERSPECTIVES OF NEUTRINO GEOSCIENCE

The two geoneutrino measurements opened a door towards a new field. It was proved that geoneutrinos can be detected and that we, as a mankind, have a new

tool how to learn new things about our planet. In order to find definitive answers to the questions correlated to the radiogenic heat and abundances of radiogenic elements, more data is needed. Both Borexino and KamLAND will continue to take data in the near future. In addition, it would be important to construct larger volume detectors in order to increase the number of detected geoneutrinos and so improve the precision of the flux measurement. Results from different detector sites placed at different geological settings is a key point for understanding, for example, if the Earth mantle composition and heat distributions are homogeneous or not. Answers to questions like what is the bulk-Earth U versus Th ratio, is it the same like in meteorites, can help in better understanding of the process of Earth formation and the distribution of elements in the Solar system. A new generation of experiments using liquid scintillators is either under the design or even in the construction process. SNO+ at Sudbury mine in Canada [30], having 1000 t of target, is in an advanced construction phase. The site is located on an old continental crust and the signal from reactor antineutrinos is about twice as the one at Gran Sasso. The main goal of the Daya Bay 2 experiment in China [31] is to determine the neutrino mass hierarchy. Thanks to a very large mass of 20 kt it would detect up to 400 geoneutrinos per year. Unfortunately, the reactor-neutrino and cosmogenic background would be the dominant sources of the systematic error. An ambitious project to construct a 50000 t detector is called LENA [32]. Among the possible sites are Pyhäsalmi in Finland or Fréjus in France. This experiment could detect of the order of 1000 geoneutrinos per year. A few percent precision of the total flux measurement could be reached within the first couple of few years. The individual contribution of the U and Th geoneutrino flux could be determined as well. An interesting project of ~ 10000 t underwater experiment is HanoHano [33] planned to be placed on the oceanic crust (Hawaii). Due to the thin oceanic crust, the mantle contribution to the total geoneutino flux should be dominant. Therefore, this measurement would provide the most direct information about the mantle. These forthcoming projects together with the currently running experiments could be a starting point of a network useful to better understand our planet.

REFERENCES

1. *Šrámek O. et al.* Geophysical and Geochemical Constraints on Geoneutrino Fluxes from Earth's Mantle // Earth and Planetary Sci. Lett. 2013. V. 361. P. 356.
2. *Rudnick R. L., Gao S.* The Crust // Treatise Geochem. V. 3. Oxford: Elsevier, 2003. P. 1–64.
3. *Huang Y. et al.* A Reference Earth Model for the Heat-Producing Elements and Associated Geoneutrino Flux // Geochem. Geophys. Geosyst. 2013. V. 14. P. 2003.
4. *McDonough W. F., Sun S.-S.* The Composition of the Earth // Chem. Geol. 1995. V. 120. P. 223.

5. *Allégre C. J. et al.* The Chemical Composition of the Earth // Earth and Planetary Sci. Lett. 1995. V. 134. P. 515.
6. *Hart S. R., Zindler A.* In Search of a Bulk Earth Composition // Chem. Geol. 1986. V. 57. P. 247.
7. *Arevalo R., McDonough W. F., Luong M.* The K/U Ratio of the Silicate Earth: Insights into Mantle Composition, Structure and Thermal Evolution // Earth and Planetary Sci. Lett. 2009. V. 278. P. 361.
8. *Palme H., O'Neill H. S. C.* The Mantle and Core // Treatise of Geochemistry. V. 2. Oxford: Elsevier, 2003. P. 1–38.
9. *Javoy M. et al.* The Chemical Composition of the Earth: Enstatite Chondrite Models // Earth and Planetary Sci. Lett. 2010. V. 293. P. 59.
10. *O'Neill H. S. C., Palme H.* Collisional Erosion and the Non-Chondritic Composition of the Terrestrial Planets // Philos. Trans. Roy. Soc. A: Math., Phys. Engin. Sci. 2008. V. 366. P. 4205–4238.
11. *Davies J. H., Davies D. R.* Earth's Surface Heat Flux // Solid Earth. 2010. V. 1. P. 5.
12. *Jaupart C., Labrosse S., Mareschal J. C.* // Treatise of Geophysics. Amsterdam: Elsevier, 2007. P. 1–53.
13. *Strumia A., Vissani F.* Precise Quasielastic Neutrino/Nucleon Cross Section // Phys. Lett. B. 2003. V. 564. P. 42.
14. *Enomoto S.* Using Neutrinos to Study the Earth: Geoneutrinos. Talk at the NeuTel 2009 Conf., Venice, Italy, 2009.
15. *Fogli G. L. et al.* Global Analysis of Neutrino Masses, Mixings, and Phases: Entering the Era of Leptonic CP Violation Searches // Phys. Rev. D. 2012. V. 86, No. 1. P. 013012.
16. *Enomoto S.* Neutrino Geophysics and Observation of Geoneutrinos at KamLAND. Ph. D. Thesis. Tohoku Univ., Japan, 2005.
17. *Araki T. et al. (KamLAND Collab.).* Experimental Investigation of Geologically Produced Antineutrinos with KamLAND // Nature. 2005. V. 436. P. 499.
18. *Abe S. et al. (KamLAND Collab.).* Precision Measurement of Neutrino Oscillation Parameters with KamLAND // Phys. Rev. Lett. 2008. V. 100. P. 221803.
19. *Bellini G. et al. (Borexino Collab.).* Observation of Geoneutrinos // Phys. Lett. B. 2010. V. 687. P. 299.
20. *Gando A. et al. (KamLAND Collab.).* Partial Radiogenic Heat Model for Earth Revealed by Geoneutrino Measurements // Nature Geosci. 2011. V. 1205. DOI:10.1038.
21. *Gando A. et al. (KamLAND Collab.).* Reactor On-Off Antineutrino Measurement with KamLAND // Phys. Rev. D. 2013. V. 88. P. 033001.
22. *Bellini G. et al. (Borexino Collab.).* Measurement of Geoneutrinos from 1353 Days of Borexino // Phys. Lett. B. 2013. V. 722. P. 295.
23. *Back H. et al. (Borexino Collab.).* Borexino Calibrations: Hardware, Methods, and Results // JINST. 2012. V. 7. P. P10018.

24. *Alimonti G. et al. (Borexino Collab.).* The Borexino Detector at the Laboratori Nazionali del Gran Sasso // Nucl. Instr. Meth. A. 2009. V. 600. P. 568.

25. *Bellini G. et al. (Borexino Collab.).* Muon and Cosmogenic Neutron Detection in Borexino // JINST. 2011. V. 6. P. P5005.

26. *Coltorti M. et al.* U and Th Content in the Central Apennines Continental Crust: A Contribution to the Determination of the Geoneutrinos Flux at LNGS // Geochim. Cosmochimica Acta. 2011. V. 75. P. 2271.

27. *Fiorentini G. et al.* Mantle Geoneutrinos in KamLAND and Borexino // Phys. Rev. D. 2012. V. 86. P. 033004.

28. *Herndon J. M., Edgerley D. A.* Background for Terrestrial Antineutrino Investigations: Radionuclide Distribution, Georeactor Fission Events, and Boundary Conditions on Fission Power Production. arXiv:hep-ph/0501216.

29. *Herndon J. M.* Substructure of the Inner Core of the Earth // Proc. Nat. Acad. Sci. USA. 1996. V. 93(2). P. 646.

30. *Chen M.* Geoneutrinos in SNO // Earth, Moon and Planets. 2006. V. 99. P. 221.

31. *Wang Z.* Update of Daya Bay II Jiangmen Antineutrino Observation Spectrometer. Talk given at the Neutrino Geoscience 2013 Conf. Takayama, Japan, 2013.

32. *Wurm M. et al.* The Next-Generation Liquid-Scintillator Neutrino Observatory LENA // Astropart. Phys. 2012. V. 35. P. 685.

33. *Learned J. G., Dye S. T., Pakvasa S.* Hanohano: A Deep Ocean Antineutrino Detector for Unique Neutrino Physics and Geophysics Studies. arXiv:0810.4975.